

## Magnetic Resonance Imaging of Biological Specimens by Electron Paramagnetic Resonance of Nitroxide Spin Labels

**Abstract.** Electron paramagnetic resonance imaging was demonstrated on two plant species, *Apium graveolens* and *Coleus blumei*. This was accomplished by soaking stems of these plants in the paramagnetic nitroxide imaging agent 4-hydroxy-2,2,6,6-tetramethylpiperidine-1-oxyl. The experiments were accomplished at L-band frequency (1.4 to 1.9 gigahertz) with single-turn, flat-loop surface coils. One-dimensional imaging spectra were diagnostic of capillary structure and long-term stability.

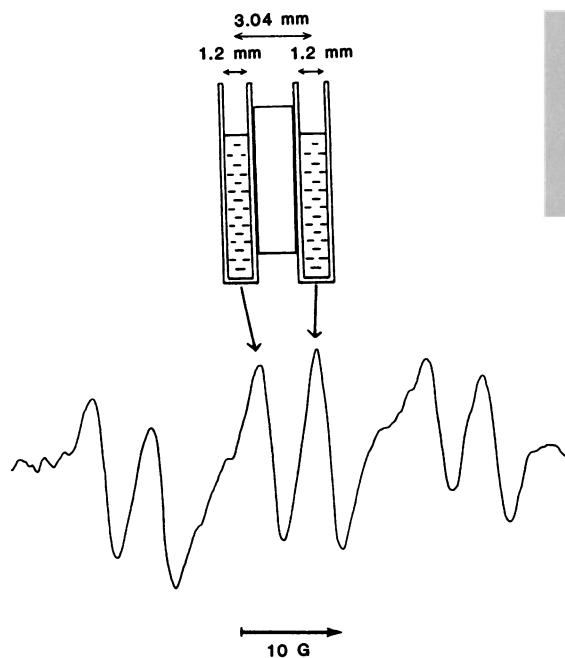
Electron paramagnetic resonance (EPR) imaging has already been used for visualizing the distribution of paramagnetic centers in materials (1). A resolved spectrum of two or more paramagnetic phantoms can be obtained in simple magnetic field gradients (2). These experiments were restricted to nondielectric materials in commercial X-band (9.5 GHz) cavities. Application of EPR imaging to living systems must overcome several problems that are obstacles with conventional spectrometer systems, namely accommodation of large sample sizes and dielectric absorption by aqueous samples (for example, heating such as occurs at X band).

We have developed a low-field EPR system at 1.4 to 1.9 GHz (L band) that has a single-turn, flat-loop surface coil (outer diameter, 0.7 to 1.0 cm) instead of a resonant cavity (3). It was found that its sensitivity equaled or exceeded that of an X-band EPR spectrometer for a typical aqueous nitroxide sample at  $10^{-6}M$ . This flat loop may be used as an EPR imaging surface coil. We constructed these surface coils with Helmholtz-type modulation coils and Maxwell pair field gradient coils set at both sides of the loop in a perpendicular arrangement (3, 4).

We report the imaging by EPR of two plant species, *Apium graveolens* (celery) and *Coleus blumei* (5), which had an aqueous nitroxide probe incorporated in their capillaries. We discuss our results from the viewpoint of vessel structure and degradative physiological phenomena in plant systems.

The spectral resolution achieved in an L-band EPR imaging experiment is illustrated in Fig. 1 for two glass capillary phantoms (inner diameter, 1.2 mm) containing 1 mM 4-hydroxy-2,2,6,6-tetramethylpiperidine-1-oxyl (TEMPOL; Aldrich) and spaced 3.04 mm apart (center to center). In the absence of a magnetic field gradient TEMPOL shows only three peaks separated by about 16 G. The six peaks shown in a magnetic field gradient of 19.4 G/cm result from the two distinct capillaries of TEMPOL. The peak-to-peak splitting between the two

sets of peaks is related to the center-to-center spacing between the two samples. This splitting increases with increasing field gradient strength; however, each three-line spectrum remains constant at



a splitting of about 16 G because of the electron-nuclear ( $^{14}N$ ) hyperfine interaction. The peak-to-peak splitting of 5.9 G corresponded to the 3.0-mm separation (center to center) between the two capillaries. We estimate that a resolution of 0.3 mm is possible.

To demonstrate the capabilities of EPR imaging *in vivo*, we applied our surface coil method to celery and coleus by introducing a paramagnetic imaging agent. Both species have many thick capillary vessels along their longitudinal axes. Figure 2 shows visualization of celery capillaries. The bottom end of a celery stalk was soaked in ink, which was rapidly transported vertically by

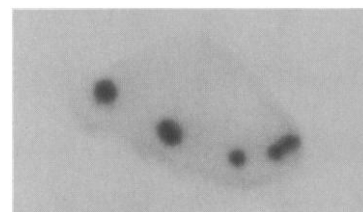
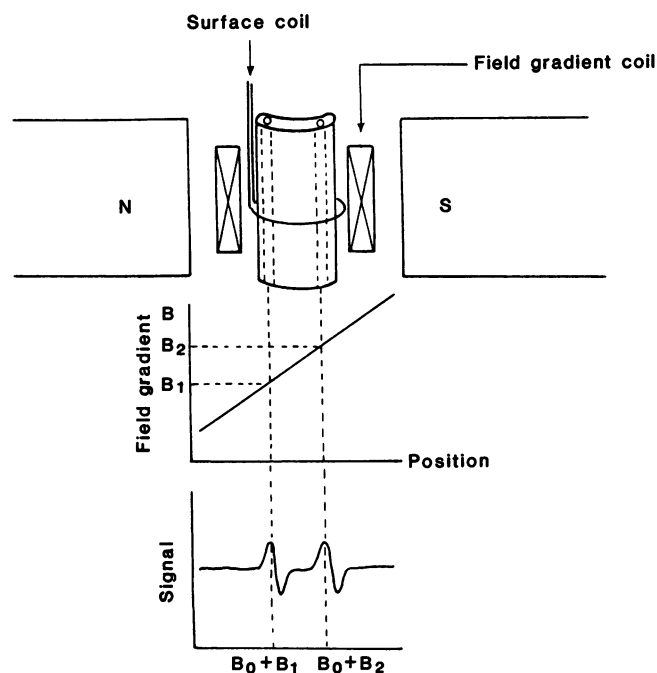


Fig. 1 (left). One-dimensional EPR spectrum of two glass capillary phantoms (inner diameter, 1.2 mm) placed 3.04 mm apart (center to center) along the  $z$  direction. Each capillary contained 1 mM TEMPOL. Microwave frequency was 1.83 GHz; applied magnetic field, 0.0660 tesla;  $z$ -field gradient, 19.4 G/cm; applied microwave power, 100 mW; and modulation frequency, 100 kHz. Fig. 2 (above). Visualization of the capillary vessels in a celery stalk after the bottom end was soaked in ink.

Fig. 3. Diagram of the one-dimensional EPR imaging experiment on a celery sample soaked in 1 mM TEMPOL. The two capillaries were aligned along the  $z$ -field gradient direction.  $B_0$  is the applied magnetic field and  $B_1$  and  $B_2$  represent the static field contribution due to the field gradient at capillary positions 1 and 2, respectively.



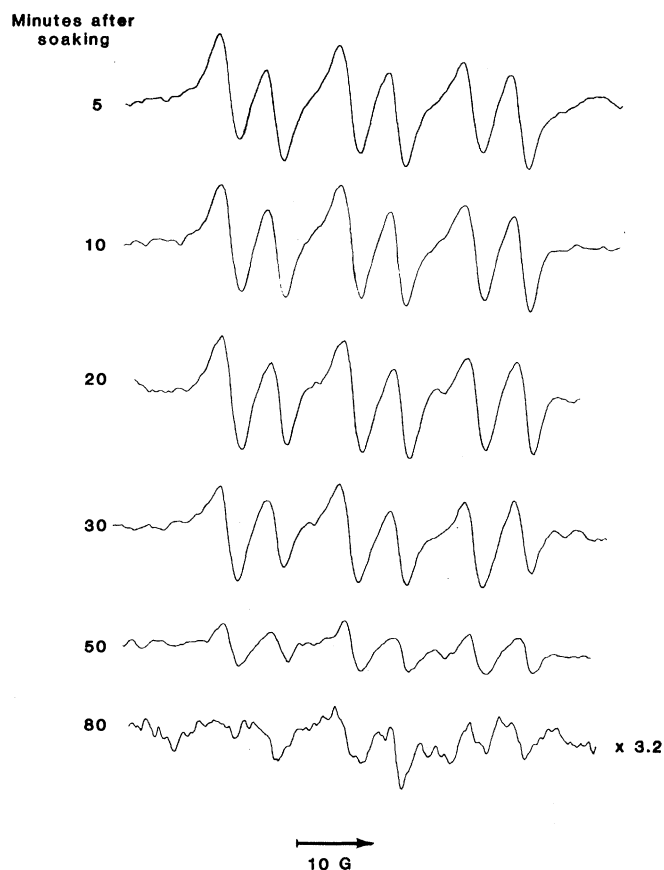


Fig. 4. Time dependence of the one-dimensional EPR spectrum of celery soaked in 1 mM TEMPOL. The  $z$  gradient was 24.3 G/cm. All other conditions were as described in the legend to Fig. 1. The two capillaries were 2.6 mm apart (center to center). After 50 minutes image resolution deteriorated with capillary breakdown and lateral diffusion of the nitroxide imaging agent.

capillary action. Figure 3 depicts an EPR imaging experiment in which a sample (2.5 cm long) of celery with only two capillaries was soaked in a 1 mM TEMPOL solution. The centers of two capillary vessels were 2.6 mm apart and their diameters were 0.8 mm. The top half of the stem was placed in the surface coil in order to monitor and image the paramagnetic material as it was drawn upward. Figure 4 shows the time dependence of this experiment. After 5 minutes we observed two strong, distinct, three-line TEMPOL spectra, that is, six peaks. One set of peaks was due to TEMPOL in the left vessel; the other set was from TEMPOL in the right vessel. After 20 minutes of soaking the TEMPOL signal intensity had reached a maximum. The splitting between the two sets of peaks was 6.2 G, which remained constant until 40 minutes after soaking. After about 50 minutes the intensity decreased with a concomitant line broadening. This was due to the migration of TEMPOL from at least one damaged vessel (by lateral diffusion) to other cellular regions. After 4 hours of soaking only one EPR signal remained (three peaks), which probably resulted from TEMPOL diffusion over the entire stem of the plant. These phenomena were observed for several samples, but the exact time

when the signal intensity maximized and diffused depended on the freshness of the celery sample.

When a 4-mm length of celery was soaked in TEMPOL solution for 20 minutes and then placed horizontal to the surface coil (the capillaries were parallel to both the applied and gradient field directions), only a single three-line TEMPOL spectrum was observed. This confirms that the vessels were uniformly occupied with TEMPOL solution and were continuous along the longitudinal axis of the celery stalk.

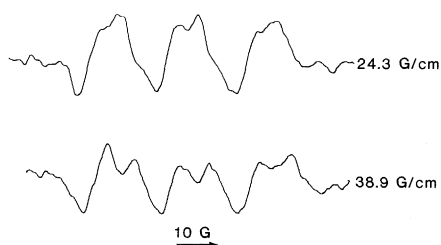


Fig. 5. One-dimensional EPR spectrum of coleus soaked in 1 mM TEMPOL at field gradients of 24.3 G/cm (top) and 38.9 G/cm (bottom). The narrow separation between capillary vessels (1.65 mm) could not be easily resolved at the lower field gradient, as is obvious by the partially resolved peaks in the top spectrum. These spectra were stable with time, signifying that there was no vessel leakage or breakdown.

Coleus has many thin vessels along the circumference of the stem which are parallel to the longitudinal axis. Samples 2.5 cm long containing just two vessels were set vertically in the surface coil and soaked in TEMPOL in the same manner as the celery. The centers of the two capillary vessels were 1.7 mm apart and the vessel diameters were 0.4 mm. Figure 5 shows spectra of coleus soaked for 10 minutes in TEMPOL. At a field gradient of 24.3 G/cm we could not resolve the spacing between two vessels, but under a gradient of 38.9 G/cm we observed two distinct sets of peaks. The EPR signals in coleus did not show the same time-dependent changes found with celery. The signal intensity and spatial resolution features were constant from at least 90 minutes to 4 hours. This meant that, since lateral diffusion of TEMPOL hardly occurred over this period, capillary vessel structure remained intact.

It is apparent that L-band EPR imaging is feasible for aqueous materials and that the prototype system described here can provide valuable information in vivo. The feasibility of detecting by EPR both naturally occurring free radicals and nitroxides in vivo has already been shown by other investigators in nonimaging modalities (6). Similar imaging applications to animal systems would be desirable.

LAWRENCE J. BERLINER  
HIROTADA FUJII

Department of Chemistry, Ohio State University, Columbus 43210

#### References and Notes

1. M. J. R. Hoch and A. R. Day, *Solid State Commun.* **30**, 211 (1979); M. J. R. Hoch, *J. Phys. C14*, 5659 (1981); K. Ohno, *J. Magn. Reson.* **49**, 56 (1982); *ibid.* **50**, 145 (1982).
2. K. Karthe and E. Wehrsdorfer, *J. Magn. Reson.* **33**, 107 (1979); T. Herrling, N. Klimes, W. Karthe, U. Ewert, B. Ebert, *ibid.* **49**, 203 (1982); O. E. Yakimchenko, I. N. Kartsivadze, B. V. Ozherelev, Y. A. Lebedev, *Dokl. Akad. Nauk SSSR* **30**, 384 (1983); S. S. Eaton and G. R. Eaton, *J. Magn. Reson.* **59**, 474 (1984).
3. H. Nishikawa, H. Fujii, L. J. Berliner, *J. Magn. Reson.*, in press; H. Fujii and L. J. Berliner, *Magn. Reson. Med.*, in press.
4. The low-field spectrometer consisted of an L-band microwave oscillator (model CC-12, KDI Electronics, Inc.; output, 100 mW), a three-port microwave circulator (model 3B1750, Microwave, Inc.), a coaxial stub stretcher tuner (Micro Lab/FXR SL-03F), a Shottky detector (HP 423B), and surface, modulation, and field gradient coils in a Varian E-4 or E-112 magnet at 0.06 to 0.07 tesla. The crystal detector was connected directly to the signal input circuit of the Varian EPR spectrometer, which also supplied the 100-kHz field modulation and frequency. The one-turn flat-loop coil was made of 0.7-mm-diameter copper wire with low-density polyethylene insulation. The outer diameter was 7 mm and the length of the coil was 41 mm for operation at 1.83 GHz. The gradient coils are Maxwell pairs (20-mm radius, 38 turns). The power supply was a Sorensen model DCR-150-12B (150 V, 12 A).
5. Celery was purchased from a local supermarket; coleus was a gift from the Department of Botany, Ohio State University.
6. S. J. Lukiewicz and S. G. Lukiewicz, *Magn.*

*Reson. Med.* 1, 297 (1983); A. Feldman, E. Wildman, G. Bartolinini, L. H. Piette, *Phys. Med. Biol.* 20, 602 (1975).

7. Supported in part by a 1-year pilot project grant (RR-02103) from NIH. We thank J. Paxton, J. Hyde, A. Heiss, R. Gerken, and J. Krauss for helpful advice and discussions. Portions of this work were presented at NMR:1984, Orlando, Fla., May 1984; the Seventh International EPR

Symposium at the 26th Rocky Mountain Conference, Denver, August 1984; the Society for Magnetic Resonance in Medicine Meetings, New York, August 1984; and the Eleventh International Conference on Magnetic Resonance in Biological Systems, Goa, India, September 1984.

10 September 1984; accepted 13 November 1984

## Two-Million-Year Record of Deuterium Depletion in Great Basin Ground Waters

**Abstract.** *Fluid inclusions in uranium series-dated calcitic veins from the southern Great Basin record a reduction of 40 per mil in the deuterium content of ground-water recharge during the Pleistocene. This variation is tentatively attributed to major uplift of the Sierra Nevada Range and the Transverse Ranges during this epoch with attendant increasing orographic depletion of deuterium from inland-bound Pacific storms.*

The mineralogy and fossil assemblages of lake beds currently provide the only tool for deciphering pre-Mid-Wisconsin paleoclimatic conditions in the Great Basin. Calcitic veins, which mark the sites of paleoground-water flow (1) within a major modern regional flow system, provide a supplementary record of paleoclimatologic and paleohydrologic events extending into the Pliocene. The calcitic veins (Fig. 1) occur in near vertical fractures in Pliocene and Pleistocene sediments at Ash Meadows, Nevada, and Furnace Creek Wash, California (Fig. 2). The veins are dense, vary from a millimeter to a meter in thickness, locally occur in swarms, and are commonly finely laminated parallel to fracture walls. They can be traced vertically for tens of meters and horizontally over hundreds of meters. Paleoclimatologic findings derived from fluid inclusions in these veins are presented here.

Veins lining opposing walls of open fractures were selected, out of hundreds of vein-sealed fractures, for both uranium-series dating and deuterium (D) analyses. Each vein was divided into groups of laminae representing the youngest (free face) to oldest (adjacent to fracture wall) portions of the vein (2). The dates of laminae of vein DH2 were calculated from  $^{230}\text{Th}/^{234}\text{U}$  activity ratios; dates of the older veins were calculated from  $^{234}\text{U}/^{238}\text{U}$  ratios (3–5). The veins range in age from about 64,000 years to 1.7 million years. Extrapolation of growth rates indicates that veins 10A and 10B may be as old as 2.6 million years.

We determined the deuterium content of fluid inclusions by using the extractive procedure of Harmon *et al.* and modifications thereof (6). Samples were heated under vacuum for 12 to 14 hours at 150°C to remove sorbed water and then were

crushed under vacuum in stainless steel tubes. Liberated water was extracted at 200°C and converted, using uranium, into hydrogen for D/H analyses. The deuterium content is expressed in parts per thousand difference (per mil) relative to standard mean ocean water (SMOW) [normalized to the V-SMOW/SLAP scale (7)]. The  $\delta\text{D}$  values are plotted against age in Fig. 2.

Fig. 1. Calcitic vein swarm, Furnace Creek Wash, Death Valley, California. Veins, which mark the routes of paleoground-water flow, occur in fanglomerate of the Pliocene Funeral Formation (17). A low-angle fault (upper third of the photo) offsets the near-vertical uranium series-dated veins at this location. Relief is on the order of 50 m at the center line of the photo.



The  $\delta\text{D}$  of fluid inclusions of late Pliocene age (laminae 10B-5 through 10B-7 and 10A-5 through 10A-8) average about  $-60$  per mil, or about 40 per mil heavier than that of modern recharge ( $-99$  per mil) and late (?) Wisconsin age (5) ground water ( $-102$  per mil) discharging today from the major artesian springs in the region (Fig. 2). More significantly, the  $\delta\text{D}$  values, in general, become progressively lighter with decreasing age over the last 1 to 2 million years. Do these values represent deuterium of Pliocene and Pleistocene ground water trapped in the veins during the calcite precipitation, or are they artifacts of (i) water-mineral exchange, (ii) remobilization of fluid inclusions during calcite recrystallization, or (iii) selective diffusion of  $^1\text{H}_2\text{O}$  from the fluid inclusions? We cannot attribute the changes in deuterium to water-mineral exchange because the water-bearing fractures in the regional carbonate aquifer, feeding the modern (and fossil) flow system, are typically coated with calcite or dolomite (8). This coating precludes the exchange of hydrogen between water and clay minerals during flow from recharge to discharge areas. In fact, the difference in